Available online at www.sciencedirect.com

SCIENCE DIRECT®

Combustion and Flame 145 (2006) 820–835

Combustion and Flame

www.elsevier.com/locate/combustflame

Effects of sample orientation on nonpiloted ignition of thin poly(methyl methacrylate) sheets by a laser
2. Experimental results

Hiroshi Gotoda [a], Samuel L. Manzello [a], Yuko Saso [b], Takashi Kashiwagi [a,*]

[a] *Fire Research Division, National Institute of Standards and Technology, Gaithersburg, MD 20899-8665, USA*
[b] *Fundamental Research Division, National Research Institute of Fire and Disaster, 3-14-1 Nakahara, Mitaka, Tokyo 181-8633, Japan*

Received 25 May 2005; received in revised form 10 January 2006; accepted 15 January 2006

Available online 9 March 2006

Abstract

The effect of the sample orientation angle on frontside (irradiated surface) ignition and subsequent backside (nonirradiated surface) flame appearance over thin poly(methyl methacrylate) (PMMA) sheets having thicknesses of 0.2 and 0.5 mm has been experimentally investigated, using a CO_2 laser as an external radiant source in quiescent normal gravity. The sample orientation angle was varied from $\theta = -90°$ (ceiling configuration) to $+90°$ (floor configuration) at intervals of 15° under three different laser powers of 16.0, 17.3, and 26.1 W. The shortest frontside ignition delay time was observed for the ceiling configuration ($\theta = -90°$) and frontside ignition delay time significantly varied with increase in sample orientation angle at a laser power of 16.0 W. As the laser power was increased, frontside ignition was observed at all angles and its delay time became less dependent on the sample orientation angle. The appearance of a backside flame was achieved after the formation of an open hole (due to local consumption of the sample) by two different processes: the onset of laser induced ignition over the backside sample (backside ignition) and a flame traveling from the frontside through an open hole to the backside (backside flame). The former process was observed for a limited number of cases only around the vertical configurations ($-30° \leqslant \theta \leqslant 30°$). The delay time for the appearance of backside flame tended to be longer for sample surfaces facing downward ($\theta° < 0$) than for the sample surface facing upward ($\theta \geqslant 0°$) regardless of the laser power. When the duration of laser irradiation was shortened from 10 to 4 s, as soon as the laser was shut off, the flame on the frontside immediately shrank, moved close to the sample surface, and then traveled rapidly to the backside. Therefore, the delay time of backside flame appearance (about 6 s) became longer with longer duration of laser irradiation after the onset of a frontside flame. The size of the hole (about 4 mm diameter) was large enough for the flame to travel through it, even after 4 s of laser irradiation to sample. These results indicate that the size of the hole appears to be not a critical parameter for the appearance of the backside flame.

Keywords: Ignition; Buoyancy; PMMA; Absorption; Sample orientation

* Corresponding author. Fax: +1 301 975 4052.
E-mail address: takashi.kashiwagi@nist.gov (T. Kashiwagi).

0010-2180/$ – see front matter
doi:10.1016/j.combustflame.2006.01.008

1. Introduction

Localized ignition of solid materials is of importance to prevent fire hazards and to understand the complex coupling of chemical, thermal, and fluid dynamics in solid combustion. Ignition is normally classified into two ignition modes: nonpiloted ignition (autoignition) and piloted ignition [1]. The former mode is induced by external radiant energy and the latter is induced by a spark, a hot wire, or a small flame near the sample surface. To investigate ignition behavior over a solid sample due to thermal radiant energy, nonpiloted ignition produced by CO_2 laser irradiation has been experimentally investigated by Kashiwagi [2]. After reaching its decomposition (i.e., pyrolysis) temperature, the sample surface heated by the incident laser irradiation evolves fuel gas consisting of degradation products due to solid-phase reactions. The evolved gas-fuel vapors strongly absorb the laser beam, which influences the ignition delay time [2,3]. Based on these experiments, many investigations by numerical or theoretical analysis have been reported for different radiant fluxes using a thermally thick sample with and without an external flow [4–8]. These investigations have demonstrated that absorption of external radiant energy by the evolved decomposition products fulfills an important role in the onset of ignition, regardless of the presence of an external flow. As the sample surface is exposed to the radiant energy, the temperature of the evolved gaseous fuel becomes high enough to undergo buoyant flow around the sample surface prior to ignition. Despite the induced buoyant flow in a normal gravity environment (especially in a quiescent environment), these previous investigations did not consider how buoyancy influences ignition behavior.

In the previous study, the effect of buoyancy on ignition behavior subjected to CO_2 laser irradiation was investigated by numerical calculation for quiescent air in normal gravity by changing sample orientation angle relative to the gravity direction (note that the laser beam is always normal to the sample surface regardless of the sample orientation angle) [9]. A change in the sample orientation angle alters the interaction between the incident laser beam and the buoyancy-induced flow consisting of decomposed products in normal gravity. This study predicted that ignition delay time would depend strongly on the sample orientation angle. At low external radiant flux, ignition occurs only when a thin sample is mounted face downward with an upward laser beam (ceiling configuration). With increasing external radiant flux, ignition occurs over a wider range of sample orientation angle. With a further increase in external radiant flux, ignition occurs at all sample orientation angles from the ceiling configuration to the floor configuration. It appears that ignition delay time tends to be longest (i.e., ignition is the most difficult to achieve) when a sample is mounted nearly vertically (a vertical sample irradiated by a horizontal laser beam).

The present study involves ignition experiments using a CO_2 laser as an external radiant source and examines the validity of these predicted results by comparing them with experimentally obtained results. It also seeks to extend current understanding of the effects of sample thickness of a relatively thin poly(methyl methacrylate) (PMMA) sheet on ignition behavior by changing the sample orientation angle. In the case of a microgravity experiment with a 0.2-mm-thick PMMA sheet [10], two separate ignition events were observed; one was ignition over the irradiated surface (*frontside*) and the other was ignition on the nonirradiated surface (*backside*). The backside ignition was achieved only after a hole through the sample was produced due to the local consumption (gasification) of the sample via continuous laser irradiation. We are interested in understanding the effects of buoyancy on the formation of backside ignition. Therefore, one of our primary interests in the present study is to investigate how buoyancy can affect ignition transition from frontside to backside through an open hole by changing the sample orientation angle in normal gravity.

2. Experimental apparatus and method

Fig. 1 shows a schematic of the experimental apparatus. A CO_2 laser (DEOS Model GEM-25)[1] with a beam diameter of about 5 mm was used as an external radiant source to ignite the sample. The total laser power Q_{ex} was varied from about 16.0 to 26.1 W (±1 W) (corresponding peak radiant flux was from 1200 to 2050 $kW/m^2 \pm 100\ kW/m^2$) and the measured radiant flux distribution was Gaussian, as shown in Fig. 2. The internal shutter was used to control both the start and the termination of laser irradiation to the sample. The sample was rotated at angles (θ) between $-90°$ and $+90°$ relative to the normal to the surface of the optical table. *The laser beam was always aligned and irradiated normal to the sample surface through the use of a rotating mirror, regardless of the sample orientation angle*. Sample orientation angle was varied from $-90°$ to $+90°$ at intervals of 15°. The sample orientation angles of $\theta = -90°$, $\theta = 0°$, and $\theta = +90°$ correspond to ceiling (horizontally placed face down configuration with an upward

[1] Certain commercial equipment, instruments, materials, services, or companies are identified in this paper in order to specify the experimental procedure adequately. This in no way implies endorsement or recommendation by NIST.

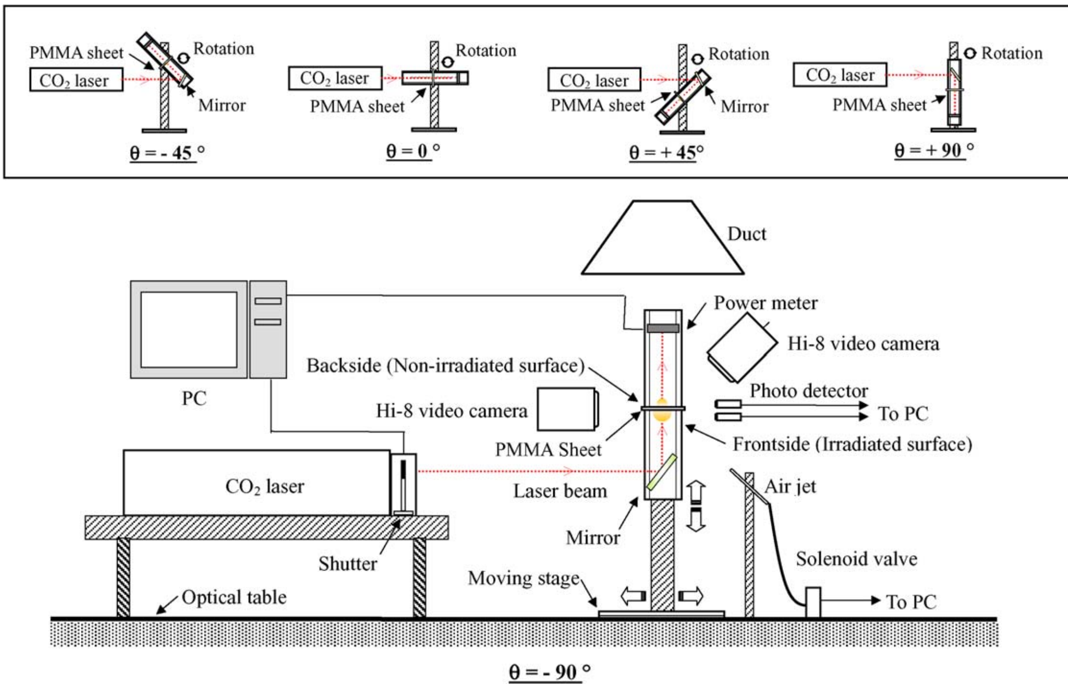

Fig. 1. Schematic illustration of the experimental setup.

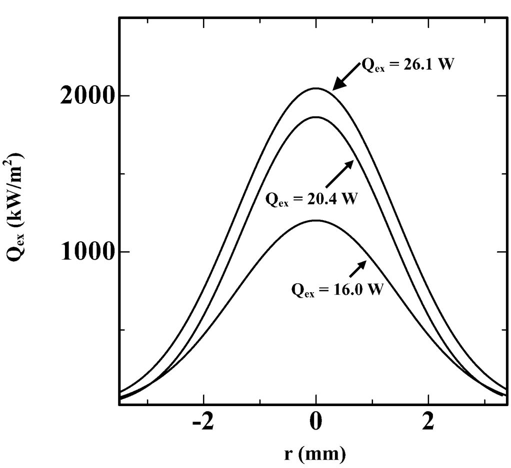

Fig. 2. Distributions of energy flux of the CO_2 laser.

laser beam), wall (vertically placed with a horizontal laser beam), and floor configurations (horizontally placed upward facing sample with a downward laser beam), respectively. The distance from the exit of the CO_2 laser to the middle of the sample was kept at 400 mm to maintain a constant laser beam diameter. A small laser power meter (OPHIR Optronics, Model 150W-A) was used well behind the sample to determine the time when a hole through the sample was formed by the local consumption of the sample, mainly due to the continuous laser irradiation. PMMA samples (Polycast, 45 mm square × 0.2 and 0.5 mm thickness δ) were used. This study focuses on the onset of frontside ignition and subsequent appearance of flame over the backside instead of flame spread along the sample. Therefore, the duration of the laser irradiation was set to 10 s regardless of whether ignition was achieved or not. This time was long enough to generate a hole up to 5 mm diameter through the PMMA samples. If, after 10 s of continuous laser irradiation, ignition was not achieved either on the irradiated surface (*frontside*) or the nonirradiated surface (*backside*) of the sample, such a test was defined as a nonignition case. To measure the onset time of ignition, two silicon detectors (Edmund Scientific, Model H55-338) were set up near the frontside and backside of the sample surface. An air jet, controlled by a solenoid valve, was applied to extinguish the flame. All features of the experiment (i.e., laser shutter, solenoid valve, and data acquisition) were controlled using a LabVIEW program. The sampling frequency of output data from both the photo detectors and power meter was 1 kHz, and the number of data points for each experiment was 10,000. In the present study, two different modes of appearance of flame over the backside were observed; one was onset of laser-induced ignition (relatively short delay from hole opening) and the other was a flame traveling through the open hole from the frontside to the backside. We define these two different modes of ap-

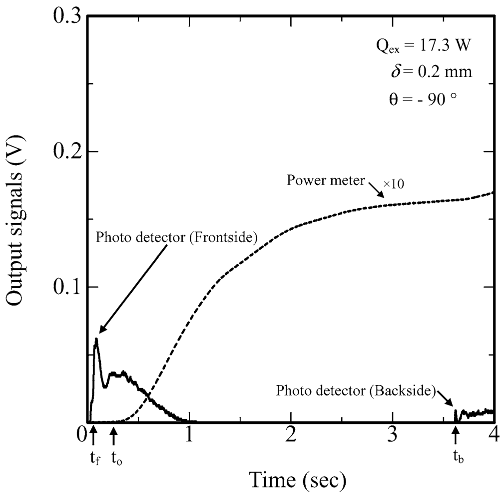

Fig. 3. Example of signal outputs from the two silicon photo detectors and the power meter with respect to time and definition of ignition delay times and a hole opening time.

pearance of the flame on the backside as "*backside ignition*" and "*backside flame*," respectively.

A typical example of the outputs of the two silicon detectors and of the power meter is shown as a function of time in Fig. 3. The time $t = 0$ is defined as the time when the sample is first exposed to the laser irradiation. When t was about 0.1 s, a sharp increase in the output of the frontside silicon detector corresponding to the onset of flaming ignition was recorded and this time was defined as the delay time of frontside ignition, t_{f}. The delay time of the backside ignition (or the backside flame), t_{b}, was also determined from the output of the second silicon detector. With respect to the power meter, the first deflection in the signal was observed at around 0.25 s (no laser beam was transmitted through the sample before the opening of a hole) and it gradually increased as the size of the hole became larger. The time at the first deflection in the signal was defined as a hole opening time, t_{o}. To obtain the images of frontside ignition and the subsequent transition to backside ignition (or backside flame) through the open hole of the sample, two Hi-8 video recorders were used at 30 frames per second. One camera recorded the frontside and backside flame behavior in a parallel view along the sample sheet. Another camera recorded a normal view of the sample surface for assessing the size of the hole.

A Schlieren visualization system was used to observe the global behavior of the thermal and degradation products plume near the sample surfaces (frontside and backside) during the ignition period. These results are used to understand the mechanism of frontside ignition and subsequent backside ignition (or backside flame) through the open hole. A schematic of the Schlieren visualization setup is shown in Fig. 4. The light source was a 10-mW He–Ne laser. A pinhole (diameter $d_{\mathrm{p}} = 0.5$ mm) was used to form a pointlike light source. The sample was mounted between two Schlieren lenses (focal length $f = 500$ mm, diameter $d_{\mathrm{l}} = 50$ mm). A Schlieren stop was set at the location of the focal point. The obtained images were captured by a compact monochromatic CCD camera (Panasonic GP-KR222) with a transmittance filter (SCHOTT) mounted directly onto the camera.

3. Experimental results

Fig. 5 shows a selected sequence of images of ignition on the frontside and the subsequent transition to flame on the sample's backside with a laser power $Q_{\mathrm{ex}} = 26.1$ W, sample thickness $\delta = 0.2$ mm, at sample orientation angles, θ, of $-90°$, $-45°$, $0°$, $+45°$, and $+90°$. At $\theta = -90°$ (ceiling configuration), a diffusion flame with a hemispherical shape was clearly observed below the sample after the onset of frontside ignition. As the sample surface continued to be irradiated by the laser beam, the size of the hemispherical diffusion flame became smaller and approached the sample surface because the supply of decomposed products (mainly methyl methacrylate, MMA) became smaller due to the local consumption of the thin sample in the narrow spot irradiated by the laser beam. A hole was formed just before the second picture frame. When the hole became large enough for the main part of the laser beam, the supply of the degradation products to the flame became limited. Then the flame became very small, with a faint color below the sample surface, as shown in the third picture frame. The energy flux from the laser irradiation was much larger than the heat feedback rate from the frontside flame to the sample before the formation of the hole. When the flame approached very close to the hole, the flame traveled through the open hole and a backside flame appeared after a delay time of about 3.5 s after the opening. At the same time as the appearance of the backside flame, the flame intensity on the frontside increased due to heat feedback from the flame on the backside. Similar flame behavior has been observed in microgravity with an external flow [10]. After the backside flame was formed, the brightness and height of the backside flame became larger with time, as shown in the fourth and fifth picture frames. This was due to the entrainment of fresh ambient air generated by the buoyancy force to the flame base on the backside.

At $\theta = -45°$, after the frontside ignition, an inclined diffusion flame was formed on the frontside and its posterior was lengthened due to the upward

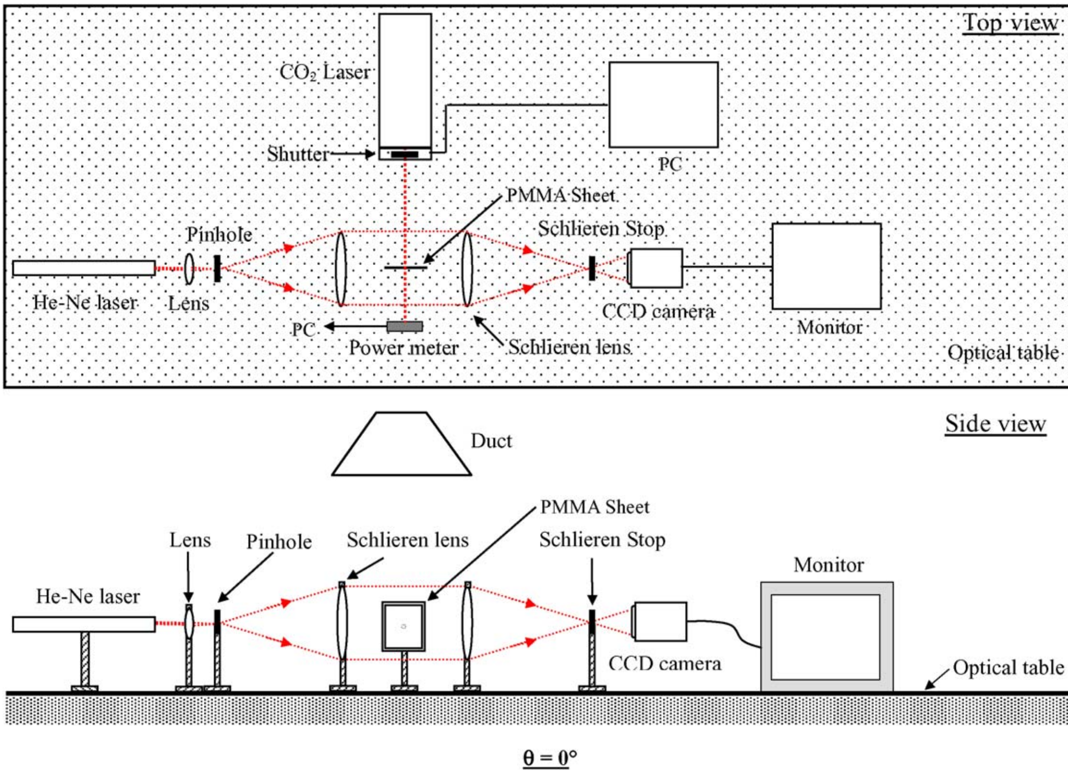

Fig. 4. Schematic illustration of the Schlieren system.

buoyancy force. Similar to that of $\theta = -90^\circ$, the size of the inclined flame became small due to local consumption of the sample after the formation of a hole due to continuous laser irradiation. After the frontside flame approached close to the open hole, a backside flame appeared through the hole with a delay time of about 4 s from the hole opening. When the sample was mounted vertically at $\theta = 0^\circ$ (wall configuration), an elongated upward flame was formed after frontside ignition. After a hole formed on the sample surface similar to that of $\theta = -90^\circ$ and $\theta = -45^\circ$, the frontside flame became small and approached close to the sample surface and the hole, and a backside flame appeared through the hole. At $\theta = +45^\circ$, after frontside ignition, a tilted diffusion flame moved close to the sample surface, but the flame was slightly away from the open hole compared with the positions for negative angles ($\theta = -90^\circ$ and $\theta = -45^\circ$) because of the upward buoyancy force. However, the backside flame was observed within 2 s from the opening of the hole. It is interesting that the transition from the frontside flame to the backside through a hole took less time at positive angles than at negative angles considering that the frontside flame stood a little away from the sample surface. At $\theta = +90^\circ$ (floor configuration), a conical diffusion flame was observed on the frontside after frontside ignition and the appearance of the backside flame took less than 2 s from the opening of a hole. The size of the backside flame remained small, probably because the flow generated by the buoyancy force caused by the frontside flame drew flow through the hole from the backside. These results indicate that the buoyancy force significantly affects the flame motions from the frontside ignition to the subsequent backside flame with different sample orientation angles.

The relationships of front ignition delay time, t_f, backside flame appearance time, t_b, and hole formation time, t_o, with respect to sample orientation angle θ are plotted at different laser powers Q_{ex} in Fig. 6. At $Q_{ex} = 16.0$ W, the frontside ignition delay time gradually increased as θ increased from -90° to -45° and ignition was achieved before the opening of a hole. When θ exceeded -45°, no frontside ignition was achieved, but an unstable boundary region, in which the frontside ignition sometimes occurred and other times did not occur, was observed at $\theta = -45^\circ$. The hole formation time t_o was nearly constant (about 0.48 s) and independent of the change in θ. With respect to the backside flame, it appeared from $\theta = -90^\circ$ to -45° with a delay of 5 to 6 s after the formation of a hole. When θ exceeded -45°, no backside flame was observed because frontside ignition was not achieved. If frontside ignition was

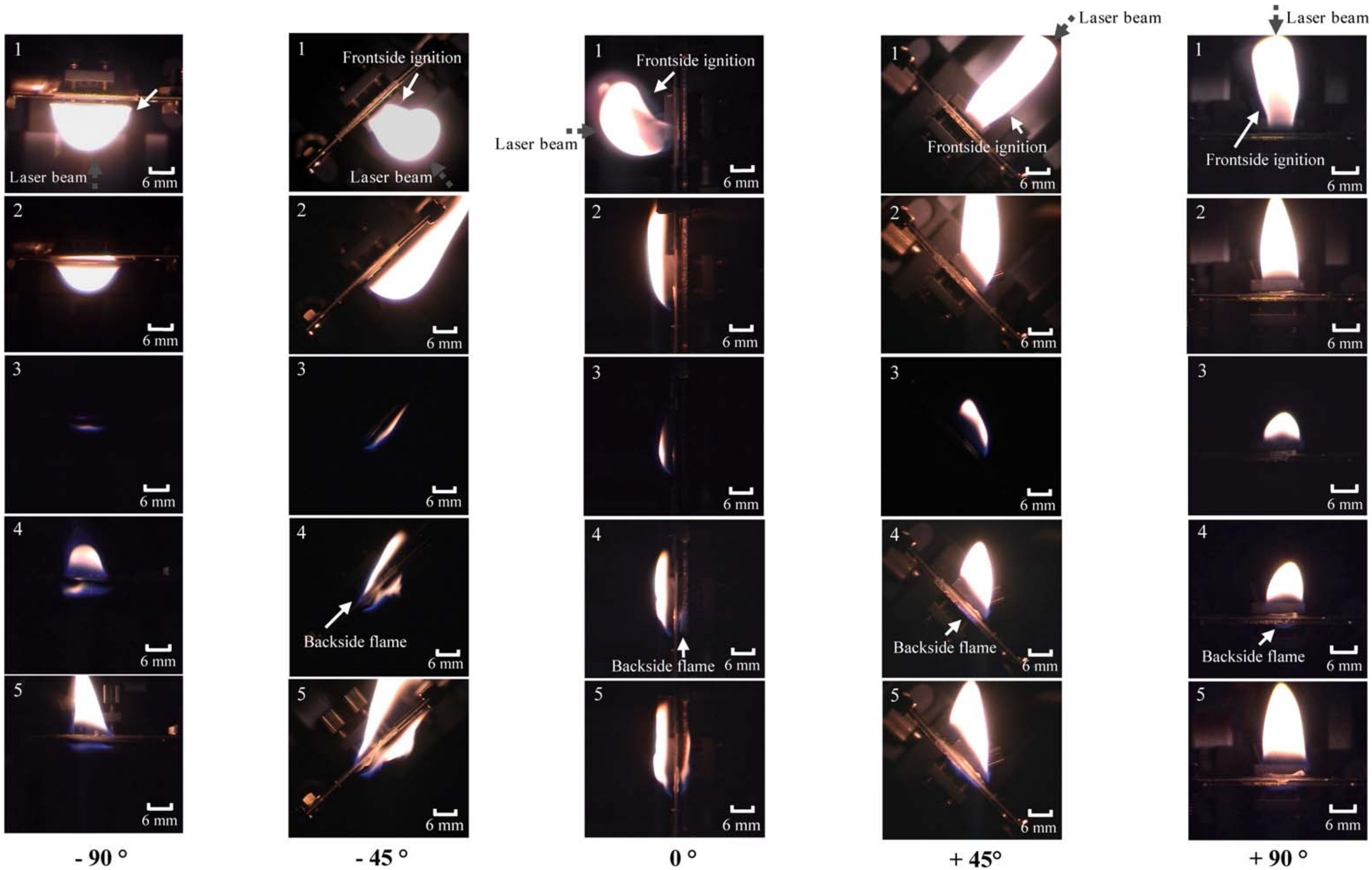

Fig. 5. Selected sequences of video images of behavior of frontside (irradiated surface) flame and appearance of backside (nonradiated surface) flame at various sample orientation angles (−90°, −45°, 0°, +45°, and +90°) for the 0.2-mm-thick sample.

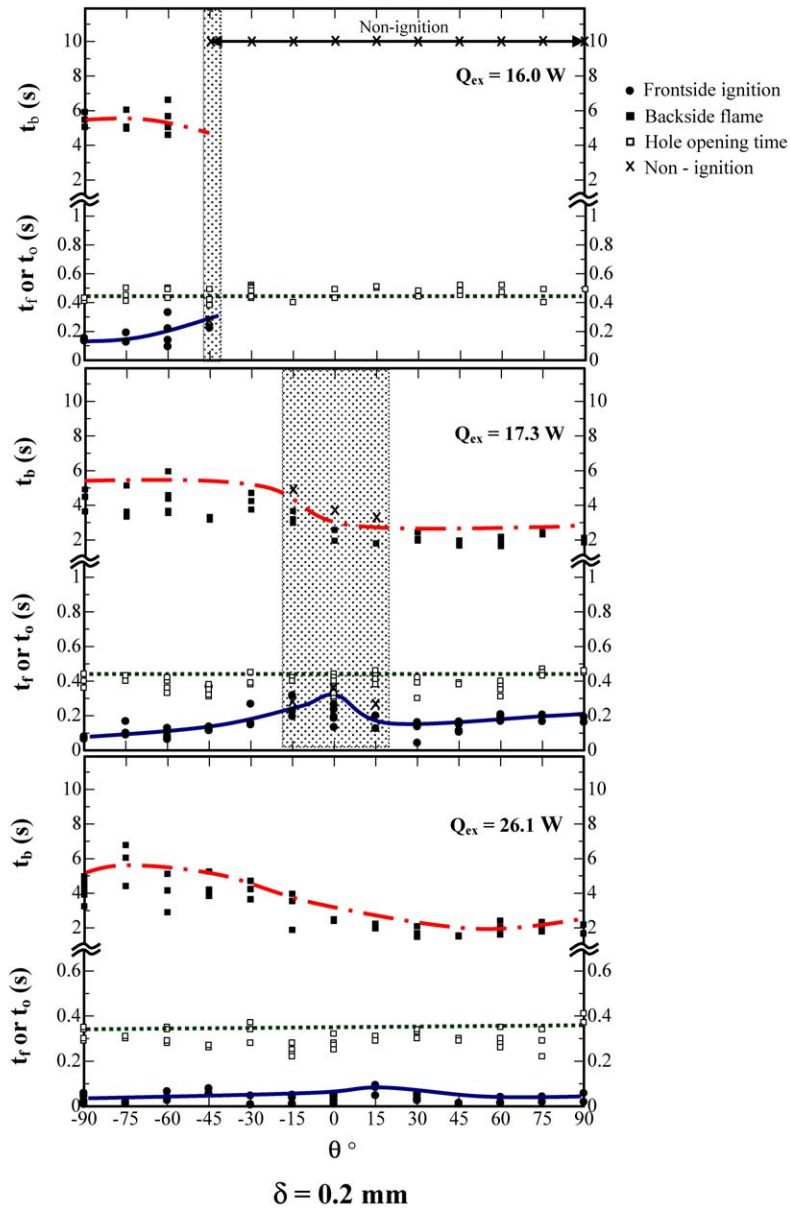

Fig. 6. Relationships of frontside ignition delay time t_f, appearance time of backside flame t_b, and hole opening time t_o with respect to the sample orientation angle θ for the 0.2-mm-thick sample. (Unstable region, shaded area, means that ignition was not achieved except in a few cases.)

achieved at $\theta > -45°$, backside flame could be attained at $\theta > -45°$.

When the laser power Q_{ex} is 17.3 W, t_f gradually increased as an increase in θ from $-90°$ to $-30°$ similar to $Q_{ex} = 16.0$ W, but the value of t_f became smaller than that of $Q_{ex} = 16.0$ W. Frontside ignition was always achieved before the opening of a hole. When θ exceeded $-15°$, the unstable boundary region similar to $Q_{ex} = 16.0$ W was observed up to $\theta = +15°$. In this region, the appearance of the backside flame depended on the occurrence of frontside ignition. With a further increase in θ, frontside ignition was always achieved. The value of t_f remained nearly constant and became insensitive to θ. The hole formation time was shorter than that for $Q_{ex} = 16.0$ W because of the higher laser energy, but it remained nearly constant regardless of θ, similarly to that of $Q_{ex} = 16.0$ W. With respect to the backside flame, t_b gradually decreased from $\theta = -90°$ to $\theta = -15°$ and then became constant (about 2 s delay from the opening of a hole) as θ exceeded $+15°$. Under conditions of higher laser power with $Q_{ex} = 26.1$ W, the frontside ignition was observed well before opening of a hole under the entire range of θ, and t_f became insensitive to θ. On the other hand, t_b gradually decreased and became constant, similarly to obtained results at lower laser energies ($Q_{ex} = 16.0$ and 17.3 W). These results indicate that the delay time of the backside flame was independent of laser power (if frontside ignition occurred over all sample angles at $Q_{ex} = 16.0$ W, the relationship between backside ignition delay time and sample orientation angle would be similar to those at $Q_{ex} = 17.3$ and 26.1 W). This trend indicates that the appearance of backside flame was due to traveling of the frontside flame through an open hole to the backside instead of the onset of ignition over the backside by laser irradiation. It was observed that the ceiling configuration ($\theta = -90°$) appears to take the shortest time to achieve frontside ignition, whereas this configuration appears to take the longest time for achieving backside flame.

Ignition and subsequent flame behavior on the frontside and the transition of the frontside flame to the backside for the samples with thickness $\delta = 0.5$ mm are shown in Fig. 7. The ignition event and the behavior of the frontside flame (large flame at the onset of ignition followed by gradual decrease in the flame size and approaching the sample surface) were very similar to those for samples with thickness 0.2 mm. Frontside ignition was achieved well before the opening of a hole except in a few cases in which ignition was observed almost at the same time as opening of a hole in the range of $-15° \leqslant \theta \leqslant +15°$ at $Q_{ex} = 16.0$ and 17.3 W. Two major differences for the samples with thickness 0.5 mm from the results with 0.2-mm-thick samples were observed: (1) the frontside flame did not travel through an open hole to the backside at negative angles ($-90°$ and $-45°$) despite the frontside flame approaching close to the sample surface and the hole regardless of continuing laser irradiation; (2) in the range $-30° \leqslant \theta \leqslant 30°$, there were two different appearances of flame on the backside after the formation of the hole: one was occasional backside ignition (as shown in Fig. 7b) and the other was no appearance of backside flame (as shown in Fig. 7a). On the other hand, for positive angles ($\theta = +45°$ and $\theta = +90°$), the backside flame was always observed after some delay (5 to 6 s after opening of a hole) and this trend was similar to that of the sample with thickness 0.2 mm (delay time of about 2 s) despite the difference in the delay time.

The relationships of frontside ignition delay time, backside flame appearance time, and hole opening time with respect to sample orientation angle at different laser power are shown in Fig. 8 for the sample of thickness 0.5 mm. At $Q_{ex} = 16.0$ W, the frontside ignition delay time monotonically increased as θ increased from $-90°$ to $0°$. As θ approached zero, frontside ignition was achieved at almost the same time as opening of a hole. Nakamura and Kashiwagi [9] predicted the same phenomena at about $\theta = -20°$ when the laser power was low. The explanation for the observation is that air supply from the backside through the open hole plays an important role in achieving frontside ignition after opening of the hole. This explanation might apply to our experimental observation but, at present, we do not have any flow measurement through the hole and we cannot confirm the predicted mechanism. Frontside ignition was achieved from $\theta = +45°$ to $\theta = +90°$, while it was not achieved with the thinner sample, as shown in Fig. 6. This indicates that the ignitable regime for frontside ignition with respect to the sample angle became larger for a thicker sample. With respect to ignition on the backside, no backside flame was observed from $\theta = -90°$ to $\theta = 0°$, even at a laser power of 26.1 W. However, the backside ignition sometimes occurred at $\theta = 0°$ after opening of a hole. In this case, the delay time of the backside ignition from opening of a hole was within 2 s, which was much shorter than for cases in which the backside flame traveled through the hole. In the regime of $0° < \theta \leqslant +45°$, no ignition was observed over either frontside or backside at $Q_{ex} = 16.0$ W. As θ exceeded $+45°$, the frontside ignition and the subsequent backside flame began to appear again and frontside ignition delay time gradually increased. The opening time of a hole remained nearly constant, except at $\theta = +90°$.

When the laser power Q_{ex} was increased to 17.3 W, frontside ignition was observed over the entire range of θ, and the trend of frontside ignition delay time with respect to θ was about the same as that for the sample of thickness 0.2 mm. Similarly to that of $Q_{ex} = 16.0$ W, no backside flame was observed for angles less than $+15°$. The backside ignition delay times after the opening of a hole were about 1 s. As θ exceeded $0°$, an unstable boundary region appeared in which the backside flame was not always achieved. Backside flame appearance time gradually decreased with an increase in θ and became nearly constant at about 5 s after opening of a hole. The regime of backside flame appearance at a laser power of 17.3 W was $+15° \leqslant \theta \leqslant +90°$ compared to $+45° \leqslant \theta \leqslant +90°$ at 16.1 W. At $Q° = 26.1$ W, frontside ignition delay time became nearly constant and did not depend on θ, similarly to that of the 0.2-mm-thick sample. Similarly to that of $Q_{ex} = 17.3$ W, no backside flame was observed from $\theta = -90°$ to $\theta = -45°$, and several cases of backside ignition were

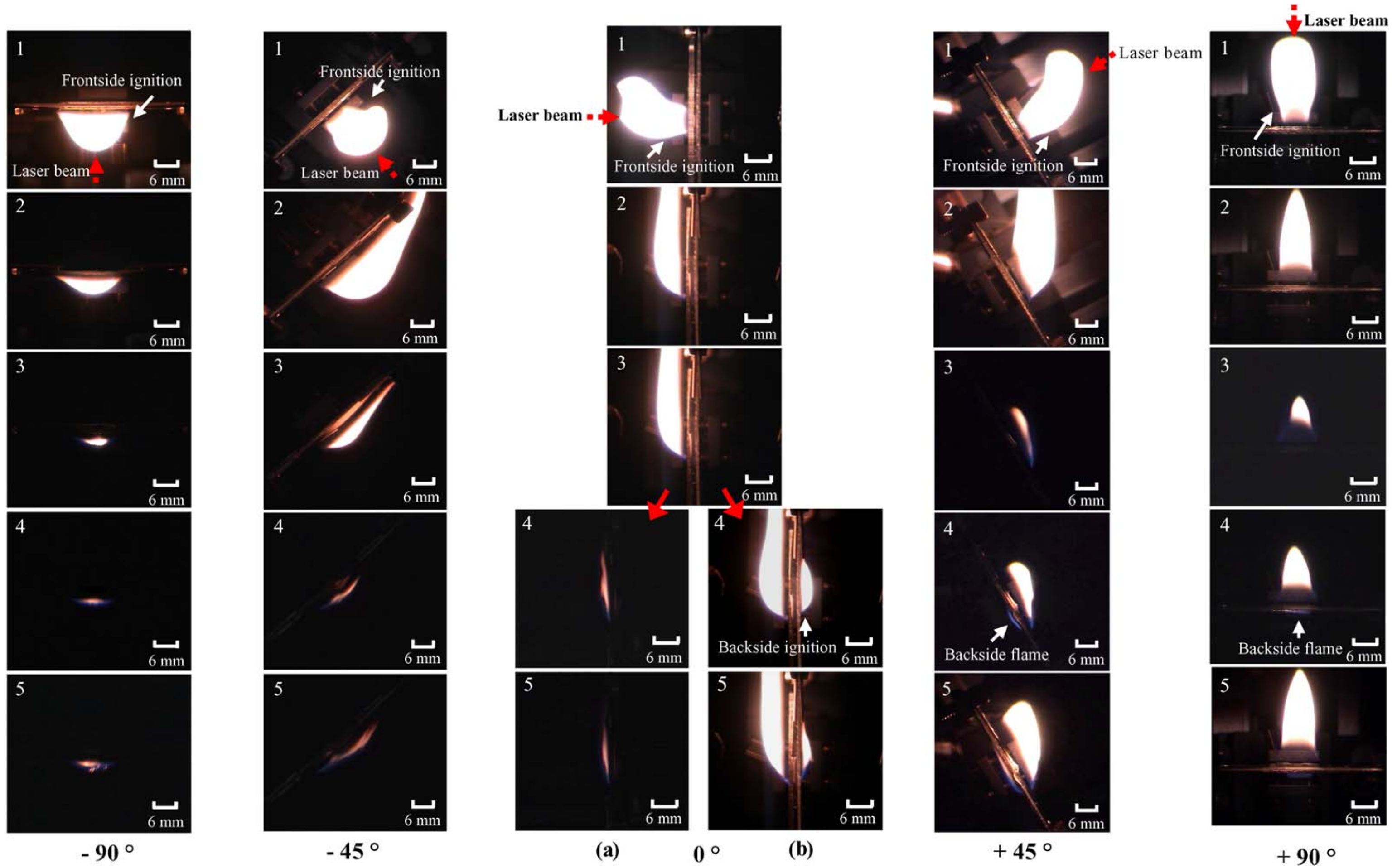

Fig. 7. Selected sequences of video images of behavior of frontside [(a) irradiated surface] flame and appearance of backside [(b) nonradiated surface] flame at various sample orientation angles (−90°, −45°, 0°, +45°, and +90°) for the 0.5-mm-thick sample.

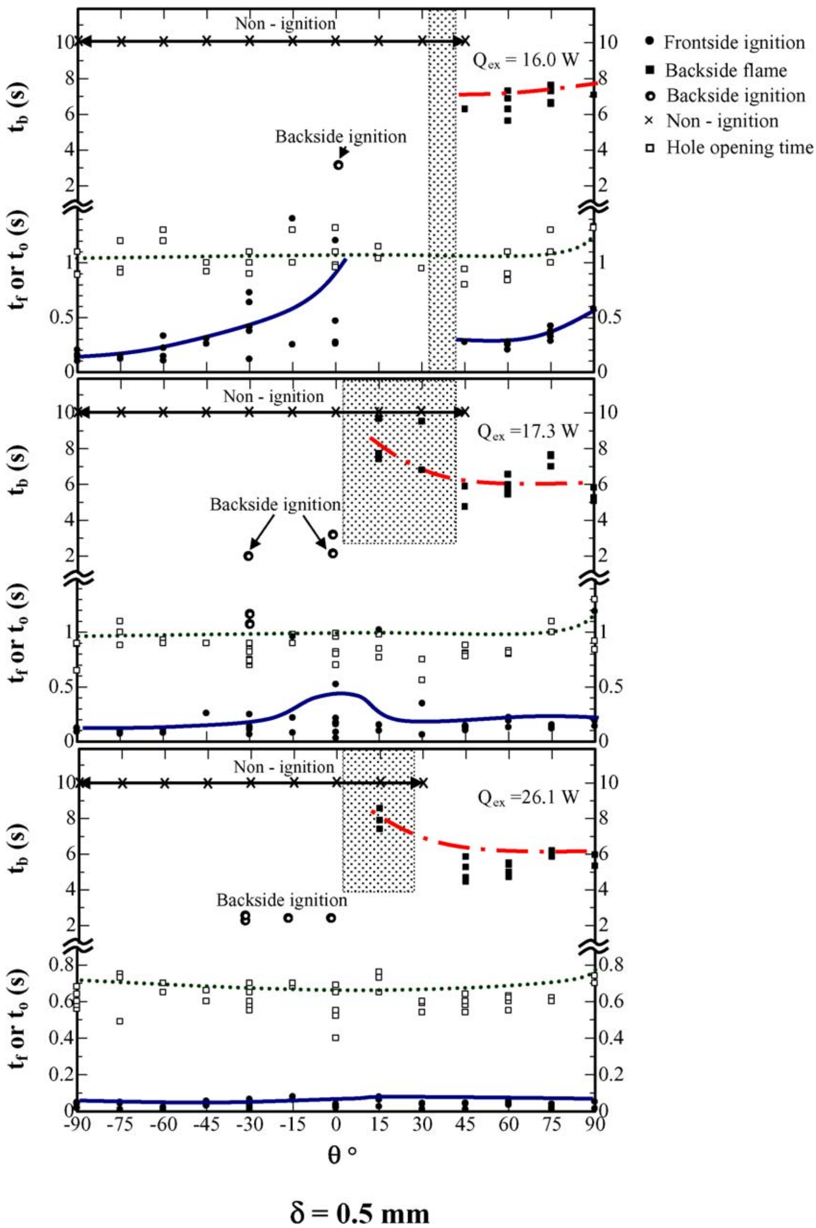

Fig. 8. Relationships of frontside ignition delay time t_f, appearance time of backside flame t_b, and hole opening time t_o with respect to the sample orientation angle θ for the 0.5-mm-thick sample. (Unstable region, shaded area, means that ignition was not achieved except few cases.)

observed for $-30^\circ \leqslant \theta \leqslant 0^\circ$. The trend of backside flame appearance time became the same as that of $Q_{ex} = 17.3$ W.

The effects of the sample thickness on the relationships of frontside ignition delay, backside flame appearance, and hole opening time with respect to the sample orientation angle at the three different laser powers are summarized as follows; frontside ignition for a thicker sample occurred over a wider range of angles than for a thinner sample at a laser power of 16.0 W. At higher laser powers, frontside ignition trend with respect to angle was similar for both samples. A backside flame was not achieved without frontside ignition for either sample. For the thinner sample, backside flame was observed over all angles at the two higher laser powers (at 16.0 W, backside flame was not observed from $\theta = -45^\circ$ to $\theta = +90^\circ$ because frontside ignition was not achieved) and tended to appear with shorter delay time from opening of a hole from $\theta = 0°$ to $\theta = +90°$. However, for a thicker sample, backside flame was not achieved from $\theta = -90°$ to $\theta = 0°$. Since buoyancy favors flow through a hole from frontside (facing downward) to backside (facing upward) from $\theta = -90°$ to $\theta = 0°$, it is unexpected that the backside flame took longer for thinner samples (no backside flame for thicker samples) from $\theta = -90°$ to $\theta = 0°$ than was the case from $\theta = +15°$ to $\theta = +90°$. From $\theta = +15°$ to $\theta = +90°$, the delay of the backside flame took about 2 s after opening of a hole for thinner samples compared to about 5 to 6 s for thicker samples. Hole-opening time did not depend on the sample orientation angle for most cases except near $\theta = +90°$ for thicker samples. As expected, hole-opening time was shorter for thinner samples and also at higher laser powers.

4. Discussion

One of the objects of this study was to examine the validity of the predicted results of frontside ignition behavior for a 0.2-mm-thick sample with respect to the sample orientation angle. The predicted results from our previous study [9] are shown in Fig. 9. The predicted frontside ignition delay time tends to be the shortest around $\theta = -90°$ and it becomes longer with an increase in the angle. The longest frontside ignition delay time tends to occur around a vertical configuration ($\theta = 0°$), and no frontside ignition is achieved at low laser powers. With further increase in the angle, frontside ignition delay time tends to decrease until $\theta \leqslant +60°$ and it slightly increases with an increase of θ over $\theta \geqslant +75°$. Similar trends of frontside ignition delay time with respect to the sample orientation angle were experimentally observed, as shown in Figs. 6 and 8. Although the experimentally measured frontside ignition delay times (0.02 to 0.4 s for the 0.2-mm-thick sample) tend to be less than those predicted (0.2–1 s), they are close to each other when one considers the use in the model of one-step global reactions for both gas-phase and condensed-phase reactions and the use of a constant absorption coefficient of gaseous MMA in the calculation. The predicted independence of hole-opening time with respect to the sample orientation angle is also confirmed by this study. The measured hole-opening times for the 0.2-mm-thick sample were in the range of 0.3 to 0.5 s compared to predicted times of 0.6 to 0.9 s. It appears that the calculated thermal degradation rates of PMMA tend to be too low or the beam absorption is underestimated. These experimental results show that, under low laser power, the ceiling case ($\theta = -90°$) is the easiest configuration for achieving

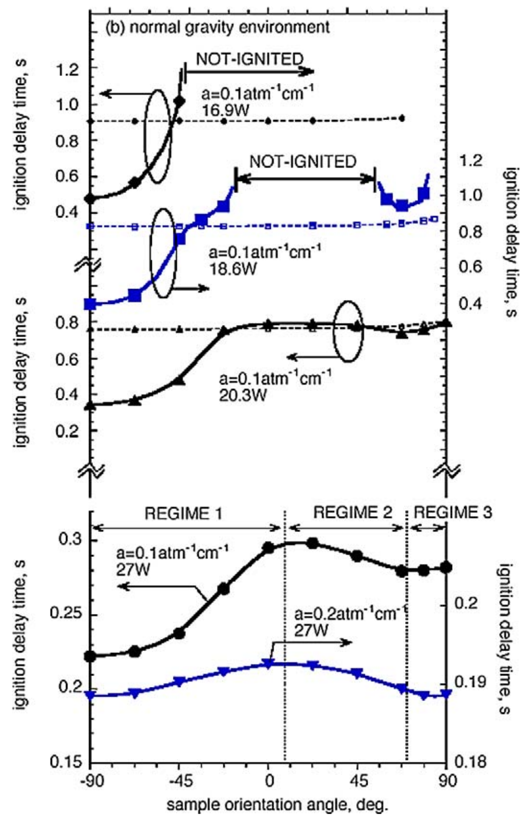

Fig. 9. Predicted relationships of frontside ignition delay time (solid line) and hole opening time (dashed line) with respect to the sample orientation angle for a 0.2-mm-sample [9].

the frontside ignition. This can be demonstrated by the finding [9] that the energy absorbed from the laser beam by MMA tends to accumulate beneath the sample surface, so that gas-phase temperature increases most rapidly to reach a runaway condition in the ceiling configuration ($\theta = -90°$) as compared with other angles.

The ignitable range of angles for frontside ignition is wider for the thicker sample than for the thinner sample at $Q_{ex} = 16.0$ W. For the thinner sample, the MMA concentration in the gas phase near the sample surface may not reach a high enough level to absorb sufficient energy from the laser beam due to local consumption of the thin sample. For a nearly vertical thin sample (0.2 mm thick), accumulation of enough MMA in the gas phase tends to become difficult with upward sweeping of MMA by the buoyancy induced flow along the surface. For the thicker sample (0.5 mm thick), there is enough sample for evolving a sufficient amount of MMA to absorb enough energy from the laser beam.

As for the mechanism of backside flame formation, the following observations should be considered. First, the frontside flame at $\theta = -90^\circ$ (ceiling configuration) was close to the sample surface due to its buoyancy, compared to that of $\theta = +90^\circ$ (the flame on the frontside was stretched away from the sample surface due to buoyancy). Second, intuitively, the upward buoyancy force makes it easier for the flame to travel from the frontside at $\theta = -90^\circ$ (facing downward) to the backside (upward facing) through the open hole. As a result, the ceiling configuration should be the easiest configuration to induce the backside flame. However, in actual fact, backside flame appearance took longer at $\theta = -90^\circ$ than at $\theta = +90^\circ$ for the 0.2-mm-thick sample. Furthermore, the backside flame was not observed for the 0.5-mm-thick sample in the ceiling configuration ($\theta = -90^\circ$) and the backside flame was observed in the floor configuration ($\theta = +90^\circ$). To clarify this unexpected result, flow visualization by the Schlieren technique was used to provide insight into the mechanism of the onset of a backside flame, including the formation of backside ignition (not backside flame) around $\theta = 0^\circ$.

Fig. 10 shows selected Schlieren image sequences near the sample surface at $Q_{ex} = 17.3$ W, $\delta = 0.5$ mm, $\theta = -90^\circ, 0^\circ, +90^\circ$. It appears that the key feature shown in the Schlieren images is the significant change in the flow of buoyant combustion products produced by the frontside flame at the three angles. At $\theta = -90^\circ$ (ceiling configuration), the combustion products and MMA were observed above the backside after hole opening. Buoyancy-induced flow of the combustion products from the frontside flame through the open hole to the backside dilutes the gas phase over the backside surface so that flame cannot travel through the hole to the backside.

At $\theta = 0^\circ$ (wall configuration), backside ignition could sometimes be achieved shortly after hole opening (no backside flame for (a) at $\theta = 0^\circ$ in Fig. 10) or, once the combustion products began to pass through the open hole, the appearance of backside flame was observed a longer time after hole opening ((b) at $\theta = 0^\circ$ in Fig. 10). (Although frontside ignition is most difficult to achieve at around $\theta = 0^\circ$ as discussed above due to upward-sweeping MMA vapor, it appears that laser energy transmitted through the thin frontside flame and then through the hole is highest, so that backside ignition initiated by the absorption of the laser energy could sometimes occur at around $\theta = 0^\circ$, as shown in Fig. 8.) At $\theta = +90^\circ$ (floor configuration), no combustion products passed through the open hole, except entrained air and MMA released from the backside to the frontside through the hole after the opening of the hole. Thus the frontside flame can travel through the hole to the backside. Therefore, it is proposed that dilution of flammable mixtures in the gas phase by combustion products significantly influences the onset of backside flame at sample angles between $\theta = -90^\circ$ and 0°. A similar mechanism can be applied to explain why the delay time of the backside flame for the $\delta = 0.2$ mm sample at $\theta = -90^\circ$ was longer than for the corresponding $\theta = +90^\circ$. It appears that the thinner sample could be expected to generate a lesser amount of combustion products due to the limited amount of the sample compared to the thicker sample. This could be why backside flame was observed for the thinner samples even at $\theta = -90^\circ$. A similar effect on flame spread due to the dilution of combustion products was observed in microgravity [11]. In the previous study, a thin paper sample was ignited (across the sample) in the middle of the sample under slow imposed flows. Initially, two flame fronts were formed; one spread upstream and the other downstream. However, the downstream flame front was not sustained due to oxygen starvation caused by the consumption of oxygen by the upstream flame and also by dilution with its combustion products. Only the upstream flame front survived and continued spreading upstream. The upstream flame phenomenon is similar to the case of backside flame at $\theta = +90^\circ$ and the downstream flame to the case at $\theta = -90^\circ$.

The growth history of the hole during the ignition experiments at various sample angles is another important piece of information for understanding the formation of backside flame. It was reported that the critical *square* hole size to allow the transition through the hole from one-sided flame spread to two-sided flame spread over a vertically mounted thin fabric was a side length of about 2 to 2.5 mm for downward spread and about 5 to 7 mm for upward flame spread [12]. The observation of hole growth in our study was, however, sometimes very difficult due to a bright frontside flame (too bright) or a small dim frontside flame (not enough light), and thus we could not always measure the hole size over the entire duration of the experiment. The timewise change of hole size at various sample angles is shown in Fig. 11 at $Q_{ex} = 17.3$ W for a 0.5-mm-thick sample. Frontside ignition (ignition delay time less than 0.5 s) was observed for all cases and backside flame was observed only at $\theta = +30^\circ$ and $\theta = +90^\circ$. Missing data points in the figure are due to too bright or too dim frontside flames as discussed above. The results show that the diameter of the hole increases rapidly to about 4 mm from about 0.8 to 4 s and then the rate of increase in the diameter slows down, reaching 6–7 mm at 10 s. The initial rapid growth of the hole up to about 4 mm diameter is mainly due to the absorption of the high energy flux from the laser, as shown in Fig. 2. At $Q_{ex} = 26.1$ W, the initial growth rate of the hole is higher than that at $Q_{ex} = 17.1$ W and the hole diameter reaches about 5 mm at about 4 s, but its growth rate

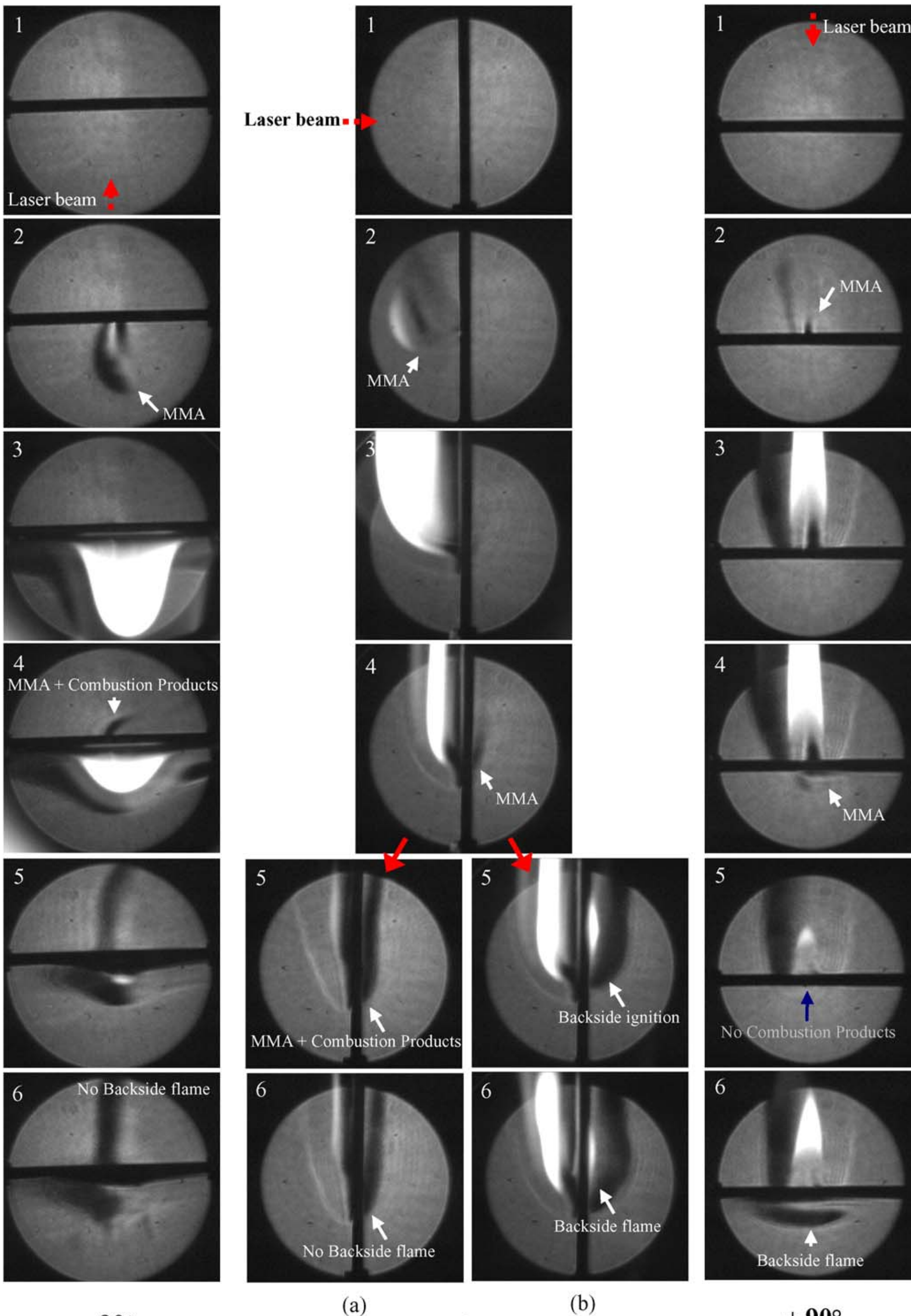

Fig. 10. Selected sequence of Schlieren images at $\theta = -90°$, $0°$ [(a) no backside flame and (b) with backside flame], and $+90°$ for the 0.5-mm-thick sample.

then becomes slightly less than that at $Q_{ex} = 17.3$ W and the diameter reaches 6–7 mm at 10 s. Backside flame appeared when the diameter of the hole was in the range from 4 to 7 mm. For a 0.2-mm sample at $Q_{ex} = 17.3$ W, backside flame was observed when the hole diameter was about 5 mm at $\theta = +30°$

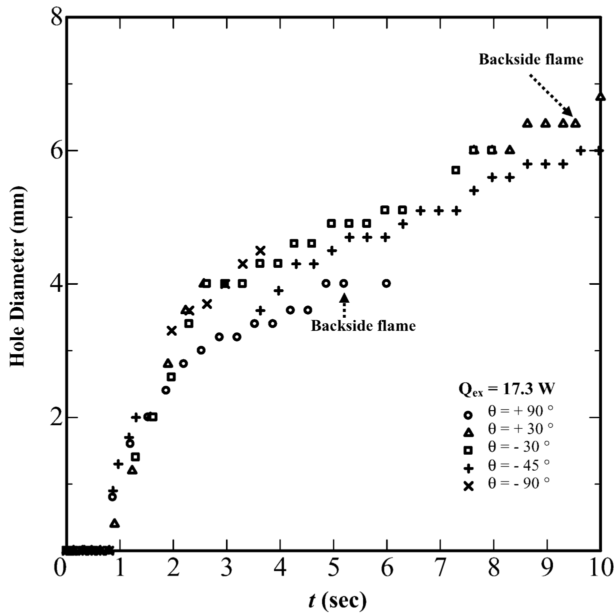

Fig. 11. The growth of a hole diameter with respect time at various sample angles for a 0.5-mm-thick sample at $Q_{ex} = 17.3$ W. (No backside flame was observed for $0 \leqslant 0°$.)

and about 7 mm at $\theta = -30°$. It is postulated that 4 to 5 mm diameter is large enough for the initiation of backside flame through a hole from the frontside flame in our study. This hypothesis is supported by the appearance of backside flame with a shorter laser duration of 4 s as described below. The validity of the proposed mechanism of dilution by the combustion products and a critical hole size for backside flame appearance will be carefully examined by numerical calculation in our next phase of study.

Microgravity experiments [10] showed that to induce the backside flame, the frontside flame had to be close to the hole when the hole was opened. This was demonstrated by turning off the laser beam shortly after frontside ignition was achieved. Although a backside flame was not observed with longer laser irradiation, a backside flame was observed with a shorter duration of laser irradiation. Therefore, it is quite possible that the duration of laser irradiation might have a significant influence on the backside flame appearance. The fuel supply rate (MMA generation rate) to the frontside flame tends to be high due to combined heat input from the laser irradiation and heat feedback from the frontside flame to the sample surface (the former is much larger than the latter). Thus, the frontside flame is pushed away from the surface and from the open hole by the high fuel-supply rate and the flame tends to be too far away from the hole. After the local consumption of PMMA in the irradiated area by continuous laser irradiation, the fuel supply rate becomes less and the frontside flame moves close to the sample and to the hole. Therefore, longer duration of laser irradiation after the onset of the frontside flame apparently can delay backside flame appearance. In order to examine this hypothesis, shorter duration of laser irradiation (4 s instead of 10 s) was used to determine the effect on the delay time of the backside flame. The results for the 0.5-mm-thick sample are shown as a function of θ in Fig. 12. From the results of Fig. 8, the backside flame did not appear until 6 to 7 s at each θ with 10-s laser duration at three different laser powers. As can be seen in Fig. 12, as soon as the laser was turned off, the flame on the frontside immediately shrank and moved close to the sample surface and to the hole due to a decrease in supply rate of MMA to the flame. Its color became a faint blue regardless of sample orientation angle. This observation supports the postulate that the critical size of the hole is about 4 to 5 mm diameter (approximate diameter at 4 s as shown in Fig. 11). The trend of a shorter laser duration is the same as that seen in microgravity experiments [11]. In a microgravity environment, the flame on the frontside was able to travel through the open hole shortly after the termination of the laser beam. However, as can be seen in Fig. 12, it could not travel through the open hole in normal gravity when θ was less than $-15°$. This is probably due to the buoyancy-induced flow of combustion products from the frontside flame through the open hole to the backside. Even though the flame immediately moved close to the hole, the backside flame could

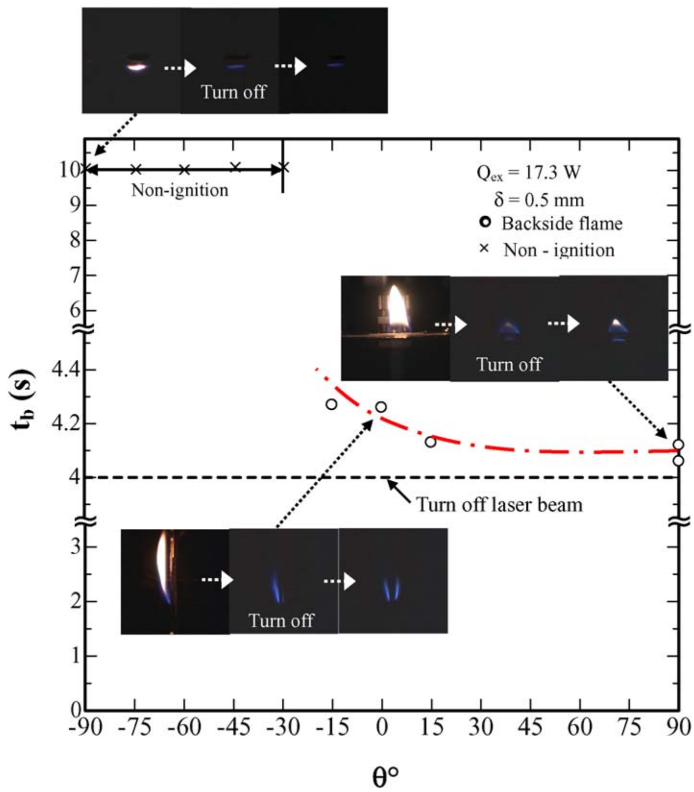

Fig. 12. Behavior of frontside flame and backside flame after turning off laser beam at 4 s and frontside ignition delay time as a function of the sample orientation angle for the 0.5-mm-thick sample.

not be achieved. When θ exceeded $-15°$, the backside flame could appear with a short delay after the frontside flame moved toward the open hole. The delay time of the backside flame gradually decreased and eventually became nearly constant with increasing θ up to $+90°$. These results indicate that the size of the hole is large enough for the flame to travel through it, even near 4 s, and the size of the hole is not a critical parameter for the appearance of the backside flame with 10 s duration of laser irradiation. These results demonstrate that the distance between the frontside flame and the open hole has a significant influence on the onset of the backside flame, not only in a microgravity environment but also in normal gravity. It is also proposed that the motion of the buoyancy-induced flow of combustion products from the frontside flame through the open hole has the predominant effect of inducing the backside flame in normal gravity, regardless of variation in the distance between the frontside flame and the hole. The proposed importance of the buoyancy-induced flow of the combustion products through the hole will be carefully examined by future numerical calculation and hopefully the results will be published as Part 3 of this study.

5. Conclusions

The effect of the sample orientation angle on frontside (irradiated surface) ignition and the subsequent appearance of backside (nonirradiated surface) flame over thin PMMA samples having thicknesses of 0.2 and 0.5 mm has been experimentally investigated using a CO_2 laser as an external radiant source in a quiescent normal gravity environment. The sample orientation angle was varied from $\theta = -90°$ (ceiling configuration) to $+90°$ (floor configuration) at an interval of 15° under three different laser powers of 16.0, 17.3, and 26.1 W.

The shortest frontside ignition delay time was observed at a ceiling configuration ($\theta = -90°$). At a laser power of 16.0 W, frontside ignition delay time increased with an increase in θ until $-45°$ for the 0.2-mm-thick sample and until 0° for the 0.5-mm-thick sample. Frontside ignition was not observed above $-45°$ for the thinner sample but it was observed above $+45°$ for the thicker sample. The smaller frontside ignition regime for the thinner sample than for the thicker sample is probably due to a limited amount of available sample (fuel vapor) for the thinner sample, which is limited by formation of an open hole through the sample due to the local consumption of the thin sample by the laser irradiation. As the laser power increased, frontside ignition was achieved before the formation of the open hole at all angles and the frontside ignition delay time became longer around $\theta = 0°$ (vertical configuration), but the delay time became less affected by the sample orientation angle. These trends of frontside ignition delay time with respect to the sample angle qualitatively agree with the results predicted by numerical simulation [9], and we confirmed the validity of the results obtained by numerical simulation.

The hole-opening time was longer with the thicker sample and at lower laser power but did not change significantly with the sample orientation angle, except for the floor configuration at 16.0 W. The appearance of the backside flame was achieved after the formation of an open hole by two different processes: the onset of laser-induced ignition over the backside sample (backside ignition) and flame traveling from the frontside flame through the open hole to the backside (backside flame). The former process was observed for a limited number of cases only around the vertical configuration ($-30° \leqslant \theta \leqslant 0°$). The delay time for the appearance of backside flame tended to be longer for the sample surface facing downward ($0° < \theta$) than for the sample surface facing upward ($\theta \geqslant 0°$) regardless of laser power. A backside flame was never observed without frontside ignition. For the 0.5-mm-thick sample, backside flame was not observed for the sample surface facing downward angles ($\theta \leqslant 0°$), even when frontside ignition was achieved. It is proposed that buoyancy-induced flow of the combustion products from the frontside flame through the open hole to the backside dilutes the gas phase over the backside surface so that flame cannot travel through the hole to the backside.

When the duration of laser irradiation was shortened from 10 s to 4 s, as soon as the laser was turned off, the flame on the frontside immediately shrank and moved close to the sample surface and it then traveled rapidly to the backside. Longer duration of laser irradiation maintained a high supply rate of MMA and pushed the frontside flame away from the hole. Therefore, the flame could not travel through the hole until the supply rate of MMA became less, due to the local consumption of PMMA over the irradiated area. Therefore, the delay time of backside flame appearance (about 6 s) became longer with longer duration of laser irradiation after the onset of frontside flame.

Acknowledgments

This study is supported by the NASA Microgravity Science Program under Interagency Agreements C-32090-K and NCC3-919. We thank Dr. Sandra L. Olson (NASA) for the use of the CO_2 laser and the laser profiler and for useful comments regarding to experimental results, and also thank Mr. John R. Shields and Mr. Marco Fernandez for helping us to make some parts of experimental apparatus. The authors thank Professor Yuji Nakamura (Hokkaido University) for useful discussion regarding the mechanism of backside flame. One of the authors (H.G.) is supported by Research Fellowships of the Japan Society for the Promotion of Science for Young Scientists.

References

[1] D. Drysdale, An Introduction to Fire Dynamics, Wiley, New York, 1985.
[2] T. Kashiwagi, Combust. Flame 34 (1979) 231.
[3] T. Kashiwagi, Combust. Flame 44 (1982) 223.
[4] B. Amos, A.C. Fernandez-Pello, Combust. Sci. Technol. 62 (1988) 331.
[5] S.H. Park, C.L. T'ien, Int. J. Heat Mass Transfer 33 (1990) 1511.
[6] C. Di Blasi, S. Crescitelli, G. Russo, G. Cinque, Combust. Flame 83 (1991) 333.
[7] T.H. Tsai, M.J. Li, I.Y. Shih, R. Jih, S.C. Wong, Combust. Flame 124 (2001) 466.
[8] T. Kashiwagi, T.J. Ohlemiller, T. Kashiwagi, Combust. Sci. Technol. 29 (1982) 15.
[9] Y. Nakamura, T. Kashiwagi, Combust. Flame 140 (2005) 149.
[10] Y. Nakamura, T. Kashiwagi, S.L. Olson, K. Nishizawa, O. Fujita, K. Ito, Proc. Combust. Inst. 30 (2005) 2319.
[11] S.L. Olson, T. Kashiwagi, O. Fujita, M. Kikuchi, K. Ito, Combust. Flame 125 (2001) 852.
[12] J. Kleinhenz, P. Ferkel, R. Pettergrew, K.R. Sacksteder, J.S. Tien, Fire Mater. 29 (2005) 27.